Nano Energy 33 (2017) 266–271

Contents lists available at ScienceDirect

Nano Energy

journal homepage: www.elsevier.com/locate/nanoen

Full paper

Can dye-sensitized solar cells generate electricity in the dark?

Qunwei Tang[a,*], Jing Wang[a], Benlin He[a], Peizhi Yang[b]

[a] Institute of Materials Science and Engineering, Ocean University of China, Qingdao 266100, PR China
[b] Key Laboratory of Advanced Technique & Preparation for Renewable Energy Materials, Ministry of Education, Yunnan Normal University, Kunming 650500, PR China

ARTICLE INFO

Keywords:
All-weather solar cell
Photoanode
Charge transfer
Energy conversion

ABSTRACT

Energy harvest requirements for future photovoltaic devices include high efficiency, cost-effectiveness, and persistent power-generation in all weathers. To address this issue, we present here all-weather dye-sensitized solar cells that can generate electricity in the daytime and in the dark by incorporating long persistence phosphors (LPPs) into mesoscopic TiO_2 (m-TiO_2) photoanodes. When suffered simulated sunlight (air mass 1.5, 100 mW cm^{-2}) illumination, the all-weather solar cell having fluorescent-emitting m-TiO_2/LPP photoanode yields a maximal photoelectric conversion efficiency of 10.08%. The unabsorbed red and infrared light across dye-sensitized m-TiO_2 layer is stored in LPP phosphors, and is subsequently converted into monochromatic fluorescence for persistent dye illumination at dark conditions, yielding a maximized photoelectric conversion efficiency up to 26.69% as well as duration lasting for several hours.

1. Introduction

Solar cells are energy harvesting devices that can convert solar energy into electricity by complicated photoelectric processes. They find multiple applications, e. g., in aerospace organizations, photovoltaic power station and photovoltaic buildings *etc.* [1–3]. Upon irradiation by sunlight, light absorbers are excited to release electron-hole pairs which are subsequently converted into electricity along charge-transfer pathways. Stepwise increase in power conversion efficiency has been realized by persistent breakthroughs in crucial materials and technologies. However, all the solar cells demonstrated so far can only generate electricity at days [4–7], while the conversion efficiencies are zero at nights. A challenge facing the development of future photovoltaic technology is to create reliable and highly efficient packaging of functional components for persistent power generation at days and nights. All-weather solar cells harvesting energy in virtually any weathers is one of the promising solutions by combining photovoltaic conversion under sunshine illumination with photoelectric conversion or energy conversion in other ways at dark conditions.

Recently, we have taken the first step to create a graphene tailored flexible dye-sensitized solar cell (DSSC) that can be triggered by rain and sun [8], generating a power conversion efficiency of 6.53% under simulated sunlight illumination (air mass 1.5, 100 mW cm^{-2}) as well as current over microamps and voltage of hundreds of microvolts by simulated rain. This graphene film is built on backward side of flexible DSSC by graphene oxide through hot-pressing and reduction processes. The low-temperature sintering generates poor contact at TiO_2/transparent conductive oxide and TiO_2/TiO_2 interfaces for electron collection and transportation along percolating mesoscopic TiO_2 (m-TiO_2) pathways [9]. To address this issue, electrophorically deposited graphene oxide [10], graphene tailored coating [11], and platinum alloys [12] were obtained on F:SnO_2 (FTO) glass substrates for sun and rain enabled bifunctional solar cells, which yielded increased photoelectric efficiencies and electrical signal outputs with reference to traditional photovoltaics. There are two limitations for abovementioned all-weather solar cells: (i) They only cover sunny and rainy days, while the power outputs are still zero at nights; (ii) The solar panels must be reversed on rainy environment, allowing for fussy operations. Therefore, it seems to be vital to invent an all-weather solar cell that can not only realize photoelectric conversion under sunlight illumination, but also create electricity at all the dark-light environments.

Here we present the experimental realization of all-weather solar cells by incorporating long persistence phosphors (LPPs) into m-TiO_2 photoanodes for unabsorbed light reutilization. LPPs are a kind of energy-storing optical materials, which could store energy from ultraviolet and/or visible light and release persistent visible fluorescence at room temperature without irradiation [13]. Due to the intrinsical light storage-excitation behaviors of m-TiO_2/LPP photoanodes, significant scientific opportunity arises from the combination of photoelectric conversion processes at days and all dark-light environments in a single solar cell device. Equally importantly, the photoelectric conversion efficiencies of launched all-weather solar cells can be significantly

* Corresponding author.
E-mail address: tangqunwei@ouc.edu.cn (Q. Tang).

http://dx.doi.org/10.1016/j.nanoen.2017.01.047
Received 8 November 2016; Received in revised form 15 January 2017; Accepted 20 January 2017
Available online 23 January 2017

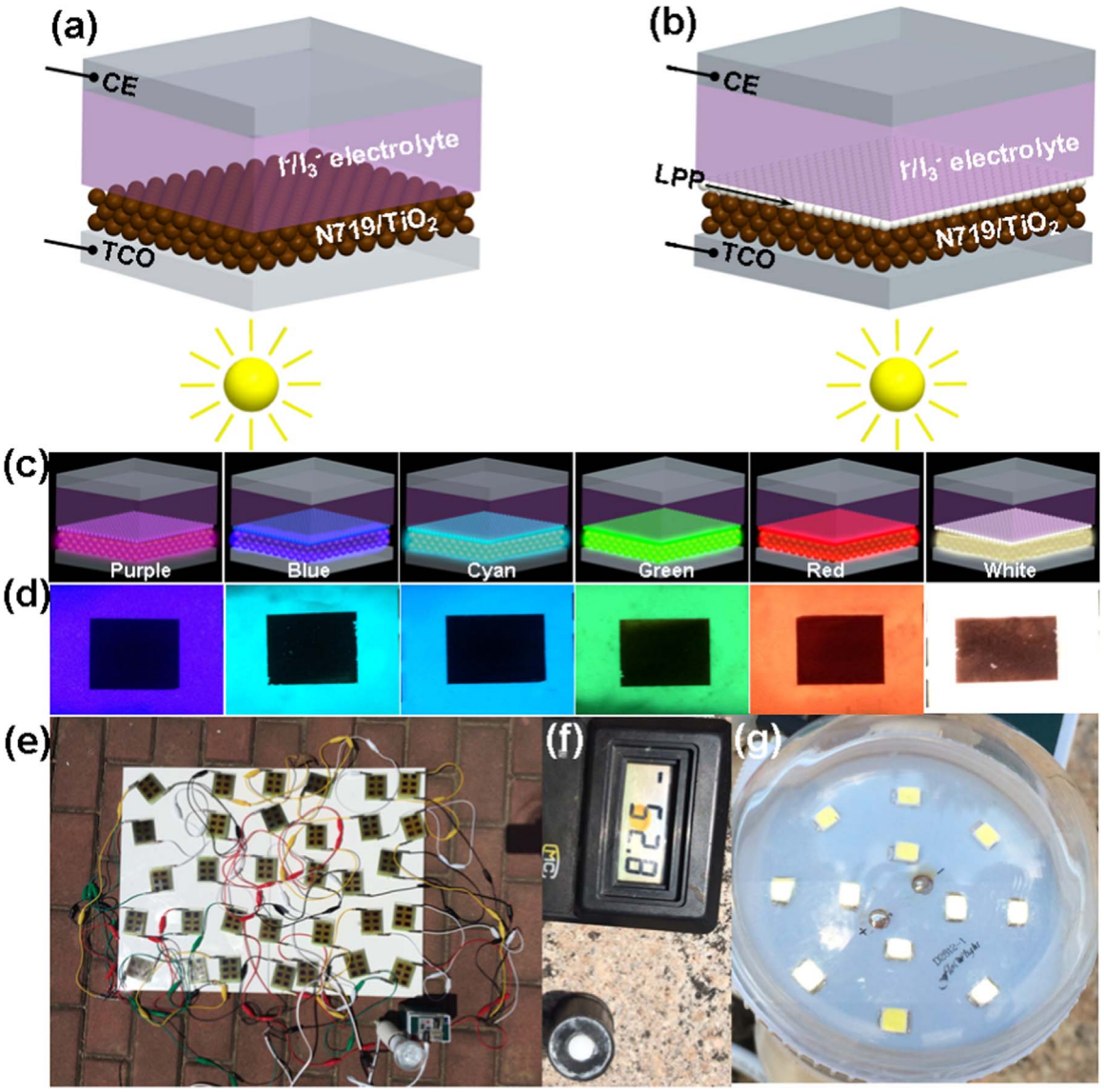

Fig. 1. (a) Sandwiched structure of state-of-the-art DSSC without LPP phosphors. (b) All-weather solar cell by incorporating LPP layer on TiO_2 photoanode. (c) Schematic diagrams of photoluminescence for all-weather solar cells at nights. (d) The photoluminescence images of six *m*-TiO_2/LPP photoanodes taken at persistent luminescence time of 5 s after irradiating by a simulated sunlight (AM1.5, 100 mW cm^{-2}) for 1 min. The dark regions are related to dye-sensitized *m*-TiO_2/LPP, while fluorescent regions are only covered by LPP layers. (e) The solar modules fabricated by 32 all-weather solar cells. (f) Recorded light intensity at outdoors. (g) The lightened light by solar modules under sun illumination at outdoors.

increased by irradiating light-absorber with monochromatic *m*-TiO_2/LPP fluorescence.

2. Experimental section

2.1. Preparation of m-TiO_2/LPP photoanodes

TiO_2 colloid was prepared according to our previous processes [14]. TiO_2 colloid was coated onto freshly cleaned FTO glass substrates (12 Ω $square^{-1}$) with size of 2×2 cm^2 by a doctor-blade method. The active area of TiO_2 layer was controlled at 0.5×0.5 cm^2 and thickness was around 10 μm. Subsequently, 0.25g mL^{-1} of LPP phosphors (purchased from Shenzhen HuiDuoSheng Luminous Material Co., Ltd.) in ethanol spin-coated onto TiO_2 layer at a rotation speed of 2000 rpm for 20 s. Finally, the FTO glass supported TiO_2/LPP films were calcined in a muffle furnace at 450 °C for 30 min in air. The resultant *m*-TiO_2/LPP photoanodes were immersed in a 0.50 mM N719 (purchased from Dyesol Australia Pty Ltd.) ethanol solution for 24 h to obtain dye-sensitized *m*-TiO_2/LPP photoanodes. The model numbers for purple, blue, cyan, green, red and white-emitting LPP phosphors were H-12B, H-10B, H-9B, H-1B, H-15B and H-13B, respectively.

2.2. Solar cell assembly

Platinum counter electrodes were prepared by a pyrolysis method. In details, a mixture consisting of 0.259 g of H_2PtCl_6, 0.2 g of OP-10 emulsifier, and 25 mL of isopropanol was dipped onto cleaned FTO glass, which was heated to 290 °C.

Each solar cell device was built by covering a platinum counter electrode with a dye-sensitized *m*-TiO_2/LPP photoanode and sealed with a Surlyn film (30 μm in thickness). A liquid electrolyte consisting of 0.1 M tetraethylammonium iodide, 0.1 M tetramethylammonium iodide, 0.1 M tetrabutylammonium iodide, 0.1 M NaI, 0.1 M KI, 0.1 M LiI, 0.05 M I_2 and 0.05 M 4-tert-butyl-pyridine was used.

2.3. Photovoltaic measurements

The photo photocurrent density-voltage (*J-V*) curves of all-weather solar cells with an active area of 0.25 cm^2 were recorded on a CHI660E

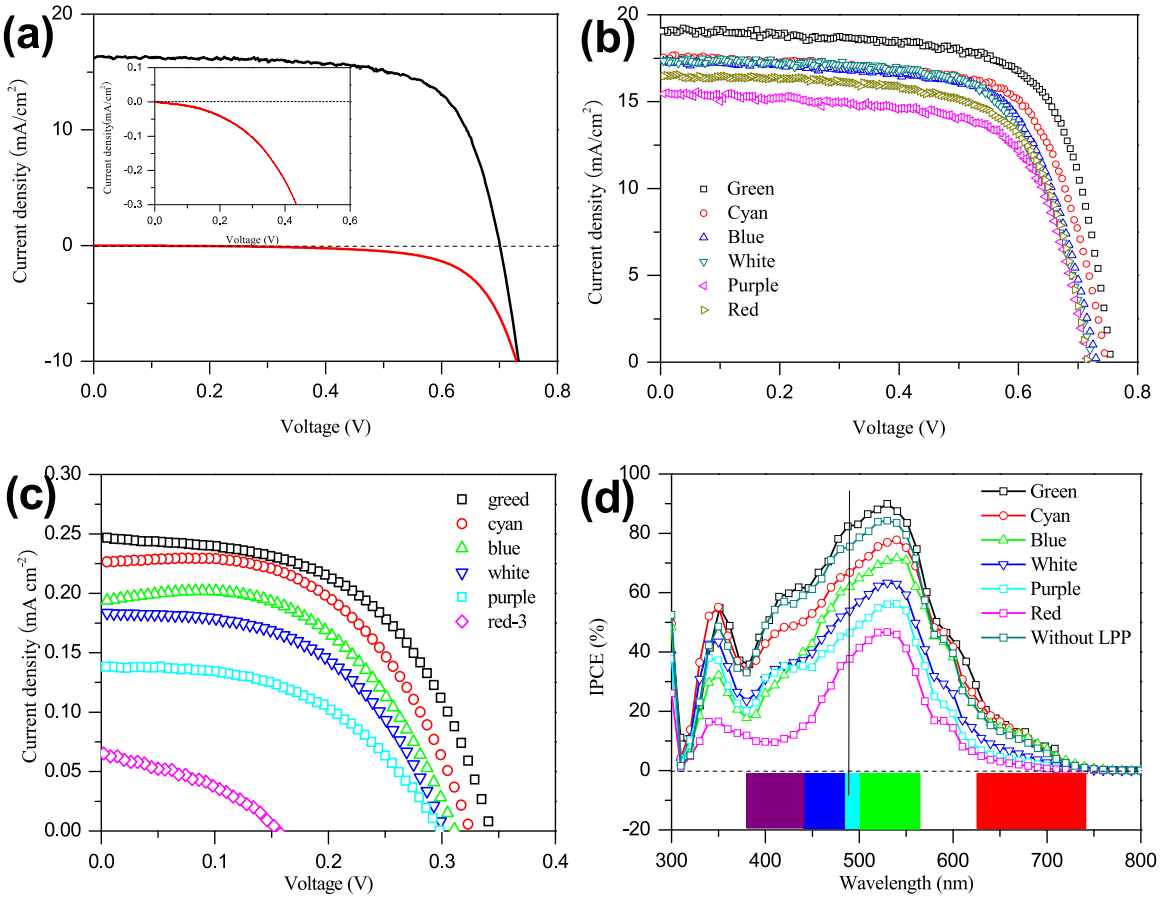

Fig. 2. (a) Representative photo and dark *J–V* characteristics of the DSSC including a dye-sensitized TiO_2 anode, a I^-/I_3^- redox electrolyte, and a Pt CE. The inset means the magnified dark *J-V* curve. (b) Characteristic photo *J–V* curves for all-weather DSSCs. An all-weather DSSC device comprises a dye-sensitized TiO_2/LPP photoanode, a I^-/I_3^- redox electrolyte, and a Pt CE. (c) The *J–V* curves for all-weather DSSCs recorded at completely dark conditions. (d) IPCE plots of the DSSCs with and without LPP phosphors. All photo *J–V* curves are measured under simulated sunlight (AM1.5, 100 mW cm^{-2}). The dark *J–V* curves are recorded in atmosphere with light intensity of 0 mW cm^{-2}.

Table 1
The photo photovoltaic parameters for corresponding solar cells. η: power conversion efficiency; V_{oc}: open-circuit voltage; J_{sc}: short-circuit current density; *FF*: fill factor.

Photoanodes	V_{oc} (V)	J_{sc} (mA cm^{-2})	η (%)	*FF* (%)
TiO_2/LPP-green	0.753	19.02	10.08	70.38
TiO_2/LPP-cyan	0.744	17.67	9.07	68.99
TiO_2/LPP-blue	0.732	17.29	8.62	68.11
TiO_2/LPP-white	0.725	17.25	8.39	67.09
TiO_2/LPP-purple	0.716	17.04	8.01	65.65
TiO_2/LPP-red	0.715	14.96	7.27	67.97
TiO_2	0.703	16.36	8.08	70.25

Table 2
The dark photovoltaic parameters for corresponding all-weather solar cells.

Photoanodes	V_{oc} (V)	J_{sc} (mA cm^{-2})	η (%)	*FF* (%)
TiO_2/LPP-green	0.343	0.247	26.69	67.66
TiO_2/LPP-cyan	0.326	0.226	22.62	67.11
TiO_2/LPP-blue	0.311	0.193	20.87	67.04
TiO_2/LPP-white	0.302	0.184	19.78	66.36
TiO_2/LPP-purple	0.298	0.138	15.35	65.77
TiO_2/LPP-red	0.157	0.065	3.02	63.05
TiO_2	0	0	0	–

electrochemical workstation under irradiation of simulated solar light from a 100 W Xenon arc lamp in ambient atmosphere. The incident light intensity was controlled to 100 mW cm^{-2} (calibrated by a standard silicon solar cell). A black mask was applied on the surface of cell device to avoid stray light. Each *J-V* curve was repeatedly obtained at least 20 times using different samples to eliminate experimental errors. Before measurement for dark *J-V* curves, the solar cells were illuminated by a simulated solar light for 1 min. Immediately, the devices were covered in a completely dark condition and the *J-V* curves were recorded on a CHI660E electrochemical workstation in air. The solar energy for dye excitation and electron generation in the dark is from fluorescence light of FTO glass supported *m*-TiO_2/LPP films, therefore, the corresponding fluorescent light intensities recorded by a standard silicon solar cell were used to calculate dark solar cell efficiency according to $\eta = P_{max}/P_{in}$, where P_{max} and P_{in} were the maximized power outputs and fluorescent intensities of *m*-TiO_2/LPP photoanodes, respectively.

3. Results and discussion

The state-of-the-art DSSC, as shown in Fig. 1a, is defined as a sandwich-structured third-generation solar cell including a dye-sensitized *m*-TiO_2 photoanode, a I^-/I_3^- redox electrolyte, and a platinum counter electrode. The photoelectronic conversion processes under sunlight illumination stem from light absorption by organic dye molecules for electron excitation. When suffering irradiation from TiO_2 anode side under a solar simulator (AM1.5 Global spectrum with 100 mW cm^{-2} intensity and spectral mismatch correction), the solar cell yields a characteristic *J–V* curve with η of 8.08% (Fig. 2a). Upon removing light irradiation, the dark *J–V* curve starts from coordinate origin, representing zero value for η, J_{sc} and V_{oc}. Upon coating with purple, blue, cyan, green, red or white-emitting LPP layer, the final *m*-TiO_2/LPP photoanodes (Fig. S1-Fig. S3) can be built to all-weather solar cells (Fig. 1b). The stacking *J–V* curves recorded under AM1.5

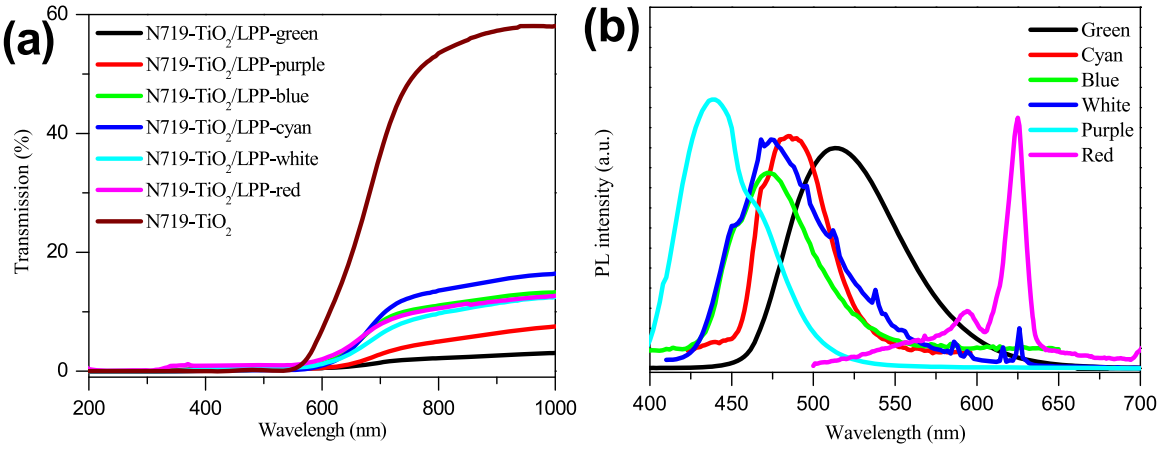

Fig. 3. (a) Optical transmission spectra of N719 sensitized *m*-TiO_2/LPP and N719 sensitized TiO_2 anodes using bared FTO glass as benchmarks. (b) PL emission spectra of *m*-TiO_2/LPP photoanodes recorded at room temperature and excited under 330 nm light excitation.

sunlight irradiation (Fig. 2b) are similar to that from pristine DSSC, and the corresponding photovoltaic parameters are summarized in Table 1. In comparison to solar cell without LPPs, the cell efficiencies are markedly enhanced from 8.08% to maximized 10.08%, arising from the incident flux from simulated sunlight and fluorescent light from LPPs. Moreover, the reduced charge-transfer resistance, as shown in Fig. S4 and Table S1, indicate that the charge-transfer processes are enhanced due to the addition of LPP layer [15]. This can be cross-checked by electrochemical impedance spectra (). Surprisingly, the recorded *J–V* curves do not pass coordinate origin at dark conditions, as shown in Fig. 2c and summarized in Table 2 generating η of 26.69%, 22.62%, 20.87%, 19.78%, 15.35%, and 3.02% for all-weather solar cells having green, cyan, blue, white, purple and red luminescence, respectively. The optimistic explanation for this would be persistent irradiation of N719 dye by persistent monochromatic luminescence from LPP phosphors [16]. As described in Fig. 1c and d, the persistent luminescence of corresponding *m*-TiO_2/LPP photoanodes can last for a long time after stoppage of excitation. In Fig. 1d, the darks for dye-sensitized TiO_2/LPP mean that colorful fluorescence can be completely absorbed by organic dyes. Notably, distinguishable red color in dye-sensitized *m*-TiO_2/red-emitting LPP suggests that not all red fluorescence is utilized. From IPCE spectrum for the DSSC without LPPs (Fig. 2d), one can find that the photovoltaics can generate electricity in the wavelengths ranging from green, cyan, blue, purple to red light. Upon incorporation with green, cyan, blue, purple, red and white-emitting LPPs, the final solar cells yield maximal IPCE values of 84%, 78%, 71%, 56%, 47% and 63%, respectively. These data are much higher than corresponding η values for traditional DSSCs by irradiating full-spectral simulated sunlight. We are inspired by this comparison to significantly enhance photoelectric conversion efficiencies of solar cells by irradiating solar cell devices with monochromatic lights. It is noteworthy to mention that the photovoltaic parameters including V_{oc}, J_{sc} and *FF* obtained in the dark are lower than that in the daytime. J_{sc} reflects the electron density at *m*-TiO_2 pathways, therefore the high light intensity under sunlight irradiation yield markedly enhanced dye excitation efficiency and electron concentration. One of the potential mechanisms behind reduced V_{oc} and *FF* is the increased electron recombination reactions in the dark conditions. A theoretical V_{oc} is defined as the energy difference between Fermi level of TiO_2 and redox potential of I^-/I_3^- couples. Upon dye excitation in the dark by emitting LPPs, the lower fluorescent light yields low electron density at TiO_2 and therefore Fermi level. On the other hand, the photogenerated electrons from front irradiation would suffer more recombination processes in comparison with rear illumination in the daytime [17].

Fig. 3a represents optical transmission spectra of N719 sensitized TiO_2 and *m*-TiO_2/LPP photoanodes using an FTO glass as a benchmark, yielding nearly zero transmissions below wavelength of 550 nm. This result suggests that almost all visible and ultraviolet light have been absorbed by N719 dye except for a tail at 550–720 nm, which can be supported by the absorption spectra in Fig. S6. Notably, there is a maximal transmission of 58% for N719 sensitized TiO_2 anode in infrared region, whereas the transmittances are reduced to 2.85%, 7.46%, 13.25%, 16.23%, 12.36%, 12.36% and 12.81% for N719 sensitized *m*-TiO_2/LPP photoanodes with green, purple, blue, cyan, white and red luminescence, respectively. From IPCE characterization, the near-infrared light at 625–720 nm has limited contributions for light excitation and therefore electricity output, not to mention the infrared light at $\lambda > 720$ nm. However, the solar energy in near-infrared and infrared regions can be reserved by LPP layer and subsequently emitted to visible light for N719 excitation according to complicated upconversion mechanisms [18]. Fig. 3b shows the emission spectra of various *m*-TiO_2/LPP photoanodes under excitation at 330 nm, green, cyan, blue and purple-emitting *m*-TiO_2/LPP photoanodes exhibit broad emissions centered at 512, 485, 464 and 438 nm, respectively. The photoanode with white luminescence yields broad emission band ranging from ~415 to ~632 nm featured with a main peak at 474 nm and associated peaks at 450, 468, 495, 511, 537, 586, 616 and 625 nm, while there are double emission peaks at 594 and 625 nm for red-luminescence anode. These emission bands indicate that the corresponding *m*-TiO_2/LPP photoanodes can emit monochromatic light by absorbing sunlight. By tuning excitation wavelengths, as shown in Fig. S7, all *m*-TiO_2/LPP anodes can convert unabsorbed light having $\lambda >$ 550 nm to corresponding visible luminescent light. Therefore, these kind of all-weather solar cells are also featured by infrared spectrum response.

Apart from above-mentioned superiorities, equally important aspect to actual efficiency of the all-weather solar cells realizing persistent electricity generation is their durability [19,20] at dark-light conditions. To demonstrate this, six *m*-TiO_2/LPP photoanodes irradiated by a simulated solar light at a light intensity of 100 mW cm^{-2} for 1 min are exposed at a completely dark atmosphere, subsequently their images are captured by a digital camera for a decay period lasting for 1 h. Fig. 4a clearly shows that all *m*-TiO_2/LPP anodes can be rapidly activated by simulated sunlight and seconds of irradiation can last for one hour of persistent visible light-luminescence emission. Only the *m*-TiO_2/LPP photoanodes for purple and red luminescences display quick darkening, arising from rapid and massive release of trapped electrons in the purchased LPPs. The potential mechanism behind the quick darkening has been detailedly described in Ref [21]. By plotting persistent luminescence intensity versus decay time for 1 h, as shown in Fig. 4b, one can find that the maximal emission intensities are 171, 176, 160, 140, 136 and 134 mW cm^{-2} for *m*-TiO_2/LPP photoanodes with green, cyan, blue, white, purple and red luminescence, respectively. Subsequently, the afterglow intensities have sharp reductions

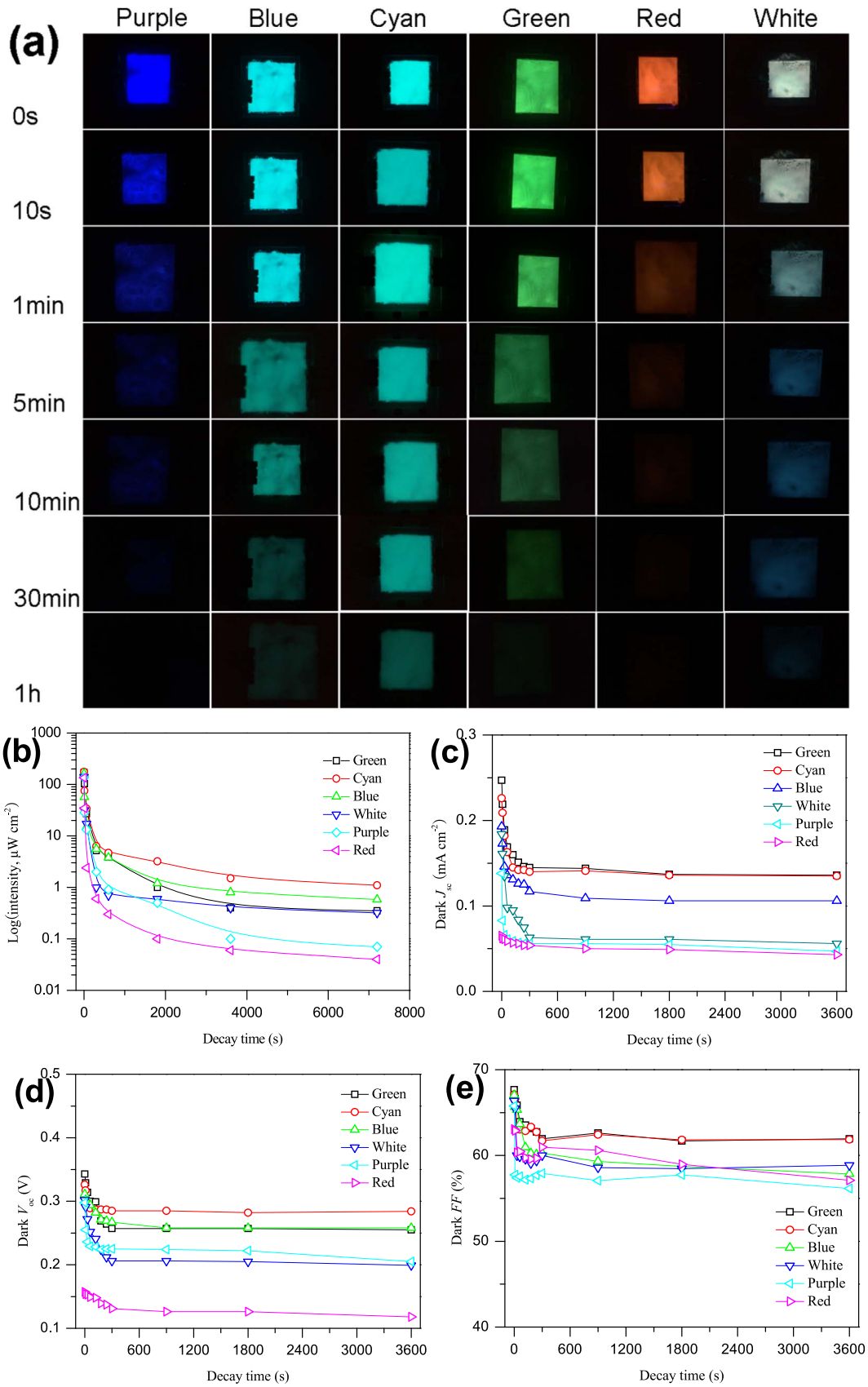

Fig. 4. (a) Images of six *m*-TiO_2/LPP photoanodes taken at different afterglow times (from 0 s to 1 h) after irradiation by a simulated solar light (100 mW cm^{-2}) for 1 min. The electrodes are not sensitized by N719 dye and average area for each photoanode is controlled at 3.6×3.8 cm^2. (b) Afterglow intensity of *m*-TiO_2/LPP photoanodes monitored by a standard silicon solar cell as a function of decay time. (c) Dark J_{sc} decay versus time. (d) Dark V_{oc} decay versus time. (e) Dark *FF* decay versus time.

within first several minutes and then decay slowly, arising from rapid energy release from LPP phosphors. In this fashion, the limited organic dye excitation leads to reduced dark photovoltaic parameters including J_{sc}, V_{oc} and *FF* (Fig. 4c-e).

To investigate the evolution of photoelectric conversion behaviors of all-weather solar cells, their dark *J-V* characteristics recorded at various decay times are shown in Fig. S8-Fig. S13 and corresponding photovoltaic parameters are summarized in Table S2-Table S7. By plotting J_{sc}, V_{oc}, *FF* or P_{max} as a function of decay time, all parameters have abrupt reductions within first 5 min and tend to nearly constants in next 55 min. By further elevating long-term stability, the all-weather solar cells could arguably realize high-efficiency electricity outputs at nights. Fundamentally, there still remain many open questions for the community concerning the solar cell efficiency under monochromatic fluorescence, high light energy storage and persistent excitation, and apply of this concept to other advanced solar cells.

4. Conclusions

In summary, all-weather solar cells that can generate electricity at days and nights are made by building *m*-TiO_2/LPP composite photoanodes. These LPPs can reabsorb the unabsorbed incident light with wavelength > 550 nm under sun illumination and subsequently emit monochromatic fluorescence for persistently exciting light-absorbers at dark conditions. Till now, six all-weather solar cells having green, cyan, blue, white, purple or red luminescence have been successfully built, yielding maximized conversion efficiency as high as 26.69% at completely dark atmosphere in comparison with 10.08% under AM1.5G irradiation. Apart from extraordinary efficiency, the launched all-weather solar cells have good long-term stability, allowing for reasonable photovoltaic performances at a decay time of one hour. Our results pave the way for further advances in all-weather solar cells.

Acknowledgements

The authors acknowledge financial supports from National Natural Science Foundation of China (21503202, 61604143, U1037604) and Shandong Provincial Natural Science Foundation (ZR2015EM024).

Appendix A. Supplementary material

Supplementary data associated with this article can be found in the online version at http://dx.doi.org/10.1016/j.nanoen.2017.01.047.

References

[1] M. Grätzel, Nature 414 (2001) 338.
[2] Q.H. Li, X. Jin, Y. Yang, H. Wang, H. Xu, Y. Cheng, T. Wei, Y. Qin, X. Luo, W. Sun, S. Luo, Adv. Funct. Mater. 26 (2016) 254.
[3] J. Du, Z. Du, J.S. Hu, Z. Pan, Q. Shen, J. Sun, D. Long, H. Dong, L. Sun, X.H. Zhong, L.J. Wan, J. Am, Chem. Soc. 138 (2016) 4201.
[4] Q.W. Tang, P.Z. Yang, J. Mater. Chem. A 4 (2016) 9730.
[5] M. Zhong, D. Xu, X. Yu, K. Huang, X. Liu, Y. Qu, Y. Xu, D.R. Yang, Nano Energy 28 (2016) 12.
[6] F. Huang, L. Jiang, A.R. Pascoe, Y. Yan, U. Bach, L. Spiccia, Y.B. Cheng, Nano Energy 27 (2016) 509.
[7] J. Chen, Y. Xiong, Y. Rong, A. Mei, Y. Sheng, P. Jiang, Y. Hu, X. Li, H.W. Han, Nano Energy 27 (2016) 130.
[8] Q.W. Tang, X.P. Wang, P.Z. Yang, B.L. He, Angew. Chem. Int. Ed. 55 (2016) 5243–5246.
[9] M.M. Maitani, Y. Tsukushi, N.D.J. Hansen, Y. Sato, D. Mochizuki, E. Suzuki, Y. Wada, Sol. Energ. Mater. Sol. C 147 (2016) 198.
[10] Y. Zhang, Q.W. Tang, B.L. He, P.Z. Yang, J. Mater. Chem. A 4 (2016) 13235.
[11] Q.W. Tang, H.N. Zhang, B.L. He, P.Z. Yang, Nano Energy, ⟨http://doi.org/10.1016/j.nanoen.2016.09.014⟩).
[12] Q.W. Tang, Y.Y. Duan, B.L. He, H.Y. Chen, Angew. Chem. Int. Ed. 55 (2016) 14412.
[13] Y. Li, M. Gecevicius, J. Qiu, Chem. Soc. Rev. 45 (2016) 2090.
[14] B.B. Hu, Q.W. Tang, B.L. He, L. Lin, H.Y. Chen, J. Power Sources 267 (2014) 445.
[15] S. Ito, S.M. Zakeeruddin, P. Comte, P. Liska, D.B. Kuang, M. Grätzel, Nat. Photonics 2 (2008) 693.
[16] Z.W. Pan, Y.Y. Lu, F. Liu, Nat. Mater. 11 (2012) 58.
[17] Y.Y. Duan, Q.W. Tang, B.L. He, R. Li, L.M. Yu, Nanoscale 6 (2014) 12601.
[18] T. Wang, W. Bian, D. Zhou, J. Qiu, X. Yu, X. Xu, J. Phys. Chem. C 119 (2015) 14047.
[19] W. Zhu, C. Bao, F. Li, T. Yu, H. Gao, Y. Yi, J. Yang, G. Fu, X. Zhou, Z.G. Zou, Nano Energy 19 (2016) 17.
[20] W. Ming, S. Chen, M.H. Du, J. Mater. Chem. A 4 (2016) 16975.
[21] W. Chen, Y. Wang, W. Zeng, S. Han, G. Li, H. Guo, Y. Li, Q. Qiang, New J. Chem. 40 (2016) 485.